Methods

FAO data

We scanned the country-level FAO data for 1995 for internal consistency, missing data and reporting errors. Missing data were assigned values using the average per capita consumption of countries in the same development category. Over-reporting because of multiple entries for the same country was corrected. For national entities or territories reporting under another administrative country, their populations were added to that of the reporting country to compute the per capita consumption. We defined consumed products as the domestic supply (that is, production plus imports minus exports) to constrain the country totals to products consumed *in situ*.

HANPP calculations

For vegetal foods and fibre, mass was successively added to account for post-harvest processing, transport losses[20,21] and crop residue[22]. Crop residue is the residue to product ratio. For the intermediate estimate we used the weighted mean for major world crops whereas high and low estimates are $\pm$ 1 s.d. (Table 1). For wood, fuel wood and paper products, organic matter was added to account for processing[23] and harvest losses[24]. For paper, recycling was also considered[25]. If the individual plant is killed (all cases except pasture) we included the biomass of the root system using the values in Table 1 (ref. 13).

Meat consumption was based on wet carcass weight and it combined all meat types. The meat component of the total HANPP was estimated by summing the NPP required for grain and pasture-based feed, assuming a global average of 62% grain and 38% forage[26]. We estimated the amount of organic matter used as feed by applying efficiency values for grain (an average of 2.3:1 kg grain/kg carcass for all meat types) and for pasture (21.46:1 for ruminants) using data from previous studies[27,28]. The total NPP required for grain feed was then calculated in the same way as for vegetal foods, adding residue and loss factors appropriate to each country's development status. Because grazing occurs *in situ*, no loss or residue factors were added to pasturage. Efficiency factors for milk and eggs are for the grain component only. Carbon/organic matter ratios used for the high, intermediate and low estimates span the range (intermediate estimate uses average value) of reported values for various plants[29].

NPP model

We used the Carnegie Ames Stanford Approach carbon model to estimate NPP. The model incorporates satellite and climate data to estimate the fixation and release of carbon based on a spatially and temporally resolved prediction of NPP in a steady state. The performance of this model is evaluated in ref. 15.

Received 6 January; accepted 5 May 2004; doi:10.1038/nature02619.

1. Vitousek, P. M., Mooney, H. A., Lubchenco, J. & Melillo, J. M. Human domination of Earth's ecosystems. *Science* **277,** 494–499 (1997).
2. Wackernagel, M. *et al.* Tracking the ecological overshoot of the human economy. *Proc. Natl Acad. Sci. USA* **99,** 9266–9271 (2002).
3. Vitousek, P. M., Ehrlich, P., Ehrlich, A. & Matson, P. M. Human appropriation of the products of photosynthesis. *Bioscience* **36,** 368–373 (1986).
4. Rojstaczer, S., Sterling, S. M. & Moore, N. J. Human appropriation of photosynthesis products. *Science* **294,** 2549–2552 (2001).
5. Schimel, D. *et al.* Contribution of increasing CO_2 and climate to carbon storage by ecosystems in the United States. *Science* **287,** 2004–2006 (2000).
6. Haberl, H. Human appropriation of net primary production as an environmental indicator: Implications for sustainable development. *Ambio* **26,** 143–146 (1997).
7. Field, C. B. Global change: Enhanced: Sharing the garden. *Science* **294,** 2490–2491 (2001).
8. Daily, G. C. *et al.* Ecosystem services: benefits supplied to human societies by natural ecosystems. *Issues Ecol.* **2,** 1–16 (1997).
9. O'Neill, R. V. & Kahn, J. R. Homo economus as a keystone species. *Bioscience* **50,** 333–337 (2000).
10. Haberl, H., Krausmann, F., Erb, K. H. & Schulz, N. B. Human appropriation of net primary production. *Science* **296,** 1968–1969 (2002).
11. Food and Agriculture Organization of the United Nations, *FAOSTAT 2001 Database* (UNFAO, Rome, 2001).
12. Center for International Earth Science Information Network, *Gridded Population of the World (GPW)* version 2 (Columbia Univ.; International Food Policy Research Institute (IFPRI); and World Resources Institute, New York, 2000).
13. Potter, C. S. *et al.* Terrestrial ecosystem production: a process model based on global satellite and surface data. *Glob. Biogeochem. Cycles* **7,** 811–841 (1993).
14. Slayback, D. A., Pinzon, J. E., Los, S. O. & Tucker, C. J. Northern hemisphere photosynthetic trends: 1982–99. *Glob. Change Biol.* **9,** 1–15 (2003).
15. Cramer, W. *et al.* Comparing global models of terrestrial primary productivity (NPP): overview and key results. *Glob. Change Biol.* **5**(Suppl. 1), 1–15 (1999).
16. Luck, M. A., Jenerette, G. D., Wu, J. G. & Grimm, N. B. The urban funnel model and spatially heterogeneous ecological footprint. *Ecosystems* **4,** 782–796 (2001).
17. van den Bergh, J. & Verbruggen, H. Spatial sustainability, trade, and indicators: an evaluation of the 'ecological footprint'. *Ecol. Econ.* **29,** 61–72 (1999).
18. Holdren, J. P. & Ehrlich, P. R. Human population and global environment. *Am. Sci.* **62,** 282–292 (1974).
19. United Nations Population Division *World Population Prospects: The 2000 Revision and The World Population in 2003* (United Nations Population Division Department of Economic and Social Affairs, New York, 2003).
20. World Resources Institute *Disappearing Food: How Big are Postharvest Losses?* (World Resources Institute Sustainable Development Information Service, Washington DC, 1998); available at ⟨http://www.wri.org/trends/foodloss.html⟩.
21. De Padua, D. B. in *Accelerating Agricultural Development* (eds Drilon, J. D. & Sanguiguit, G. F.) 135–154 (SERCA College, Laguna, 1978).
22. Smil, V. *Biomass Energies: Resources, Links, Constraints* (Plenum, New York, 1983).
23. Ince, P. J. *Industrial Wood Productivity in the United States 1900–1998* (Research Note FPL-RN-0272, USDA Forest Service, Madison, 2000).
24. Pulkki, R. E. *Literature Synthesis on Logging Impacts in Moist Tropical Forests* (working paper GFSS/WP/06, Forest Products Division, UNFAO, Rome, 1997).
25. Skog, K. E., Ince, P. J. & Haynes, R. W. Wood fiber supply and demand in the United States. *Proc. N. Am. For. Comm.* [online] ⟨http://www.fpl.fs.fed.us/documnts/pdf2000/skog00a.pdf⟩, 1998.
26. Sere, C. & Steinfeld, H. *World Livestock Production Systems* (Animal Production and Health Paper 127, FAO, Rome, 1996); available at ⟨http://www.fao.org/WAICENT/FAOINFO/AGRICULT/AGA/LSPA/Paper127/cover1.htm⟩.
27. Council for Agricultural Science and Technology, *Animal Agriculture and Global Food Supply* (Task Force Report R135, Ames, 1999); available at ⟨http://www.cast-science.org/cast/pub/anag_nr.htm⟩.
28. Oltjen, J. W., George, M. R. & Drake, D. J. in *Computers in Agricultural Extension Program* (eds Watson, D. G., Zazuelta, F. S. & Bottcher, A. B.) 58–63 (American Society of Agricultural Engineers, St Joseph, 1992).
29. Lieth, H. in *Primary Productivity of the Biosphere* (eds Lieth, H. & Whittaker, R. H.) 119–130 (Springer, New York, 1975).

Acknowledgements We thank K. Carney, N. Christiansen, G. Daily, R. Defries, J. Hellmann, J. Hicke, G. Orians, N. Sanders, P. Vitousek, P. Matson and P. Ehrlich for comments, C. Tucker for providing satellite data, and G. Asrar, J. Kaye, G. Gutman and D. Wickland of the US National Aeronautics and Space Administration for financial support.

Competing interests statement The authors declare that they have no competing financial interests.

Correspondence and requests for materials should be addressed to M.L.I. (Marc.L.Imhoff@nasa.gov).

A proteoglycan mediates inductive interaction during plant vascular development

Hiroyasu Motose[1]*, Munetaka Sugiyama[2] & Hiroo Fukuda[1,3]

[1]*Department of Biological Sciences, Graduate School of Science, The University of Tokyo, Hongo 7-3-1, Bunkyo-ku, Tokyo 113-0033, Japan*
[2]*Botanical Gardens, Graduate School of Science, The University of Tokyo, Hakusan 3-7-1, Bunkyo-ku, Tokyo 112-0001, Japan*
[3]*Plant Science Center, RIKEN, Suehiro 1-7-22, Tsurumi-ku, Yokohama, Kanagawa 230-0045, Japan*

* Present address: Section of Plant Biology, Division of Biological Sciences, University of California, One Shields Avenue, Davis, California 95616, USA

Inductive cell–cell interactions are essential for controlling cell fate determination in both plants and animals[1]; however, the chemical basis of inductive signals in plants remains little understood. A proteoglycan-like factor named xylogen mediates local and inductive cell–cell interactions required for xylem differentiation in *Zinnia* cells cultured *in vitro*[2,3]. Here we describe the purification of xylogen and cloning of its complementary DNA, and present evidence for its role *in planta*. The polypeptide backbone of xylogen is a hybrid-type molecule with properties of both arabinogalactan proteins and nonspecific lipid-transfer proteins. Xylogen predominantly accumulates in the meristem, procambium and xylem. In the xylem, xylogen has a polar localization in the cell walls of differentiating tracheary elements. Double knockouts of *Arabidopsis* lacking both genes that encode xylogen proteins show defects in vascular development: discontinuous veins, improperly interconnected vessel elements and simplified venation. Our results suggest that the polar secretion of xylogen draws neighbouring cells into the pathway of vascular differentiation to direct continuous vascular development, thereby identifying a molecule that mediates an inductive cell–cell interaction involved in plant tissue differentiation.

The plant vascular system, comprised of xylem and phloem, forms a continuous network throughout the plant body to transport water, nutrients and signalling molecules. Vascular cells differentiate

by contact with each other to form a continuous strand of vasculature. This developmental feature of the vascular system has raised the possibility that some inductive signals function to guide continuous vascular differentiation. Such inductive signals have not been defined, however, in part because of difficulties in analysing cell–cell interactions *in planta*. *In vitro* xylogenesis of *Zinnia* (*Zinnia elegans* L.)[4,5] offers an excellent experimental system for directly analysing cell–cell interactions and for isolating signal molecules. In this culture system, isolated mesophyll cells of *Zinnia* transdifferentiate into tracheary elements (TEs), distinctive cells composing xylem vessels *in planta* that are characterized by the formation of secondary cell wall thickenings and programmed cell death. Our previous investigation with this culture system suggested that premature TEs draw neighbouring cells into the pathway of TE differentiation[2]. This inductive cell–cell interaction was found to be mediated by a locally acting secretory factor, which was named xylogen for its xylogenic activity. The activity of xylogen in the conditioned medium of *Zinnia* xylogenic culture was recovered in the fraction of arabinogalactan proteins (AGPs), a group of plant proteoglycans[3].

We purified xylogen from the AGP fraction by using concanavalin A affinity chromatography after a boil treatment. Purified xylogen increased the frequency of TE differentiation in *Zinnia* cell culture, whereas chemically deglycosylated xylogen did not (Fig. 1a–c), indicating that the glycosyl chains of xylogen are required for its activity. Notably, xylogen derived from the dicot *Zinnia* could promote TE differentiation from mesophyll cells of the monocot *Asparagus officinalis* L. (Fig. 1d–f), suggesting that xylogen is not species-specific but is common to diverse angiosperms. SDS polyacrylamide gel electrophoresis (SDS–PAGE) of purified xylogen yielded a broad band with a relative molecular mass of 50,000–100,000 (M_r 50K–100K), whereas deglycosylated xylogen migrated as a sharp band with an M_r of 16K (Fig. 1g). No other protein bands were detected by silver staining, indicating the homogeneity of the purified xylogen. Monoclonal antibody JIM13 and β-glucosyl Yariv reagent (βGlcY), which detect AGPs[6,7], bound to purified xylogen but not to deglycosylated xylogen (Fig. 1g), consistent with reports that JIM13 and βGlcY recognize the glycosyl chains of AGPs[6,8]. Addition of βGlcY to the *Zinnia* cell culture potently suppressed TE differentiation as compared with α-galactosyl Yariv reagent (αGalY), an inactive analogue of βGlcY (Fig. 1h). From these results, we conclude that xylogen is an AGP that is essential for TE differentiation.

Amino-terminal amino acid sequencing of the 16K deglycosylated xylogen gave the sequence AHQTGAOAOAADCSTVILNM (where O is hydroxyproline). On the basis of this information, a cDNA encoding xylogen was generated by rapid amplification of cDNA ends (RACE). The resulting cDNA had an open reading frame (ORF) of 183 amino acids, which contained the amino acid sequence identical to the N-terminal sequence determined for deglycosylated xylogen (Fig. 2a). The gene represented by this cDNA is designated *Z. elegans xylogen protein 1* (*ZeXYP1*). Analysis *in silico* indicated that ZeXYP1 is a hybrid-type molecule with properties of both AGPs and nonspecific lipid-transfer proteins (nsLTPs).

Four domains can be recognized in the sequence of ZeXYP1 (Fig. 2b): an N-terminal signal peptide, an nsLTP domain, a proline–alanine (Pro-Ala)-rich domain, and a predicted glycosyl phosphatidylinositol (GPI)-anchor attachment site followed by a carboxy-terminal transmembrane region. The nsLTP domain contains eight cysteine residues, which are strictly conserved in plant nsLTPs and form four disulfide bridges[9,10]. ZeXYP1 shares two characteristics with the polypeptide backbones of AGPs: a GPI-anchor signal that is conserved in a large family of AGPs[11–13], and short runs of proline alternating with alanine or threonine[14] (APAPA just before the nsLTP domain and APTPA in the (Pro-Ala)-rich domain). On the basis of AGP structure[14], two proline residues of APAPA, which were shown to be hydroxylated, are probably *O*-linked to arabinogalactans. The binding of xylogen to concanavalin A suggests that an *N*-glycan side chain containing mannose residues is present at the one potential *N*-glycosylation site.

Two homologous genes of *Arabidopsis thaliana*, At5g64080 and At2g13820, were identified by a BLAST search with *ZeXYP1* as a query and designated *A. thaliana xylogen protein 1* (*AtXYP1*) and

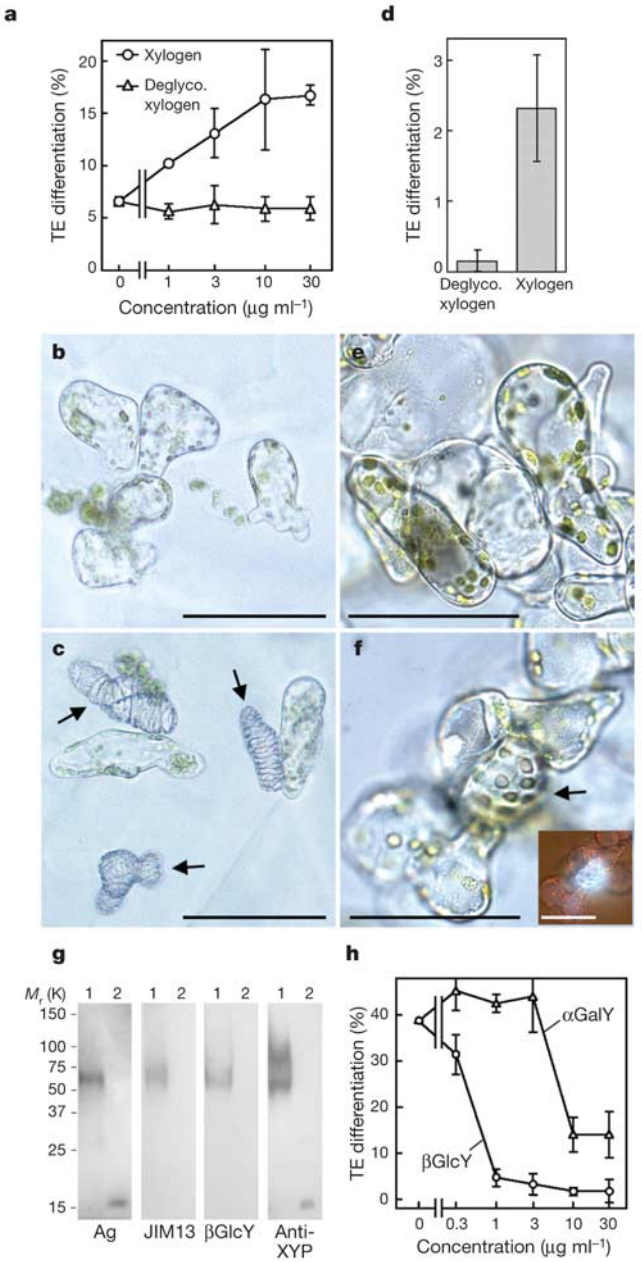

Figure 1 Xylogen is an arabinogalactan protein that induces xylem differentiation. **a**–**f**, Xylogen induces tracheary element (TE^{-1}) differentiation of *Zinnia* (**a**–**c**) and *Asparagus* (**d**–**f**) mesophyll cells. *Zinnia* cells were cultured with 30 μg ml^{-1} deglycosylated xylogen (**b**) or 30 μg ml^{-1} xylogen (**c**). *Asparagus* cells were cultured with 30 μg ml^{-1} deglycosylated xylogen (**e**) or 30 μg ml^{-1} xylogen (**f**). Arrows indicate TEs (**c**, **f**). Inset in **f** shows an ultraviolet image indicating lignin deposition in a TE. Scale bar, 50 μm (**b**, **c**, **e**, **f**). **g**, Electrophoretograms of xylogen (lane 1) and deglycosylated xylogen (lane 2). Samples separated by SDS–PAGE were stained with silver (Ag), or blotted onto nitrocellulose membranes and stained with JIM13, βGlcY or anti-ZeXYP1 antibodies. **h**, βGlcY inhibits TE differentiation in *Zinnia* suspension culture.

AtXYP2, respectively. ZeXYP1, AtXYP1 and AtXYP2 have a conserved domain organization (Fig. 2b), with the exception that AtXYP2 has no putative *N*-glycosylation site. The three proteins share significant identity in their nsLTP domains (60.5% identity; Fig. 2a). To test functionally whether *ZeXYP1*, *AtXYP1* and *AtXYP2* encode xylogen, we overexpressed these genes and analysed their effects on the activity of xylogen. Overexpression of *ZeXYP1*, *AtXYP1* or *AtXYP2* under the control of cauliflower mosaic virus 35S promoter in tobacco BY-2 cells resulted in the accumulation of xylogen in culture media (Fig. 2c) and in marked increases in xylogen activity (Fig. 2d), verifying that these genes encode the polypeptide backbones of xylogen. Notably, the production of AtXYP2 with no *N*-glycosylation site increased the activity of xylogen similarly to the production of ZeXYP1 and AtXYP1. This suggests that *N*-glycosylation is not required for the activity of xylogen.

Xylogen was isolated as a diffusible apoplastic factor from the conditioned medium; however, the putative GPI-anchor attachment site found in the amino acid sequences of xylogen proteins suggested that these proteins are tethered to the plasma membrane. Immunoblot analysis indicated that ZeXYP1 accumulated in the conditioned medium, with no detectable ZeXYP1 in the microsomal fraction (Fig. 2e). A possible explanation for these results is that xylogen is released from the membrane by GPI-anchor cleavage phospholipases, as has been reported for AGPs of *Nicotiana alata*[11], *Pyrus communis*[11,12] and *Rosa*[13]. This issue should be addressed by a more detailed analysis.

In general, nsLTPs interact with lipids and sterols and enhance their *in vitro* transfer between membranes[9,10]. The ability of xylogen to bind lipids and sterols was therefore assessed by a protein–lipid overlay assay (ref. 15 and Methods). Purified xylogen preferentially bound to stigmasterol and weakly bound to brassicasterol among the steroids and fatty acids tested (Fig. 2f). This result suggests the possibility that xylogen functions as a sterol–proteoglycan complex. Deglycosylation of xylogen had no effect on the sterol-binding ability of xylogen (Fig. 2f), indicating that the interaction between xylogen and sterols depends on the protein moiety of xylogen.

We next examined the accumulation pattern of xylogen during TE differentiation of *Zinnia* mesophyll cells (Fig. 3a–d). The *ZeXYP1* transcripts started to accumulate 24 h before visible formation of TEs and peaked at 48 h of culture (Fig. 3a). Immunoblot analysis showed that xylogen accumulated in the culture medium 12 h before visible TE formation (Fig. 3c). The period of accumulation of xylogen corresponds to stage II of xylogenesis[5], during which dedifferentiated cells restrict their competence and become precursors of TEs. Because auxin and cytokinin are essential for TE differentiation, we evaluated their effects on the accumulation of xylogen. The accumulation of the *ZeXYP1* transcripts was induced

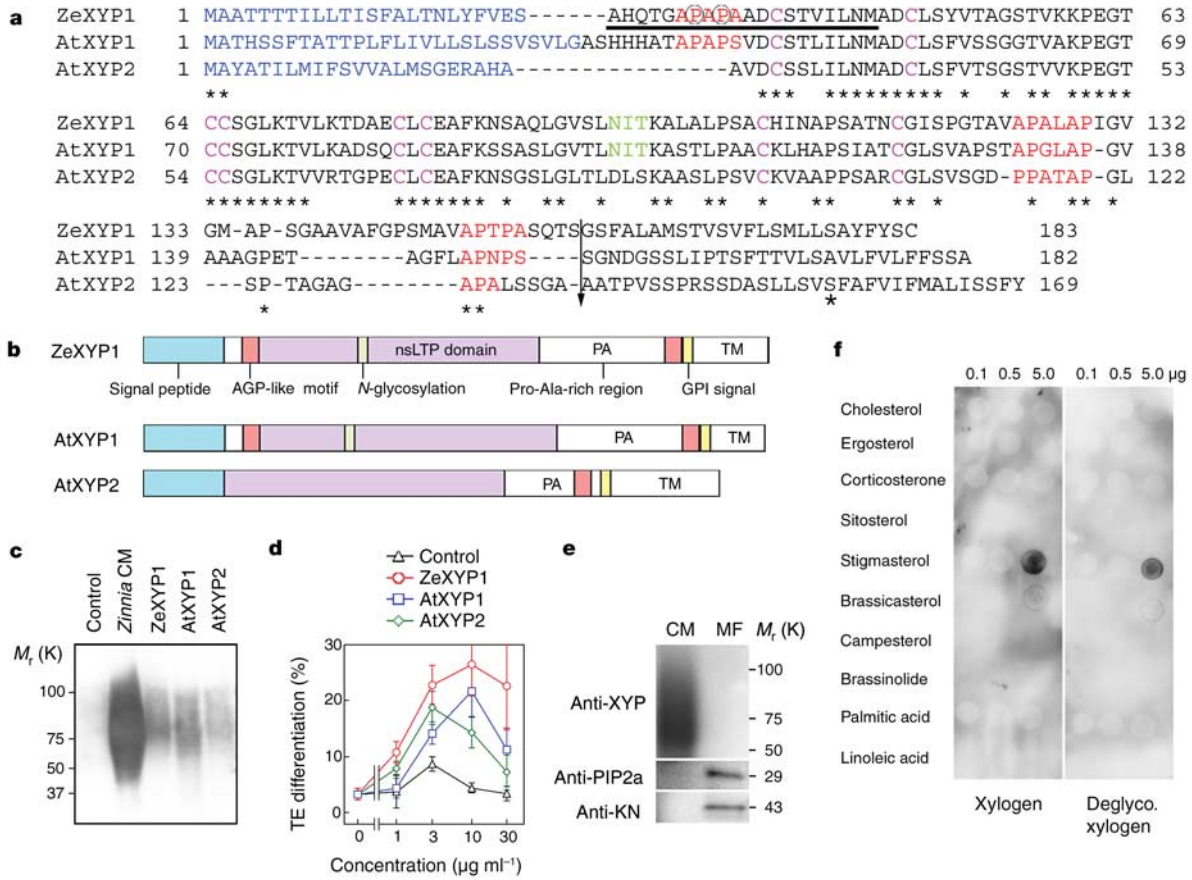

Figure 2 Characterization of xylogen. **a**, Deduced amino acid sequences. Shown are the signal sequences (blue), AGP-like motifs (red), nsLTP-like cysteines (purple), *N*-glycosylation sites (green), identical residues (asterisks), cleavage sites followed by the GPI anchor (arrow), sequenced N-terminal amino acids (underlined) and hydroxylated prolines (circles). **b**, Domain structures of xylogen. PA, (Pro-Ala)-rich domain; TM, transmembrane domain. **c**, Transgenic BY-2 cells overexpressing *ZeXYP1*, *AtXYP1* or *AtXYP2* accumulate xylogen, as detected by a protein gel blot analysis with anti-ZeXYP1 antibody. *Zinnia* CM, conditioned medium of *Zinnia* xylogenic culture. **d**, Activity of xylogen of transgenic BY-2 cells measured with a *Zinnia* microbead culture. **e**, Immunoblotting of conditioned medium (CM) or microsomal fraction (MF) of *Zinnia* xylogenic culture detected by antibodies against ZeXYP1 (XYP), PIP2a or KNOLLE (KN). **f**, Selective binding of xylogen to sterols in a protein–sterol overlay assay.

by auxin (Fig. 3a, b), whereas both auxin and cytokinin were required for the accumulation of xylogen (Fig. 3c, d). These results indicate that the accumulation of xylogen is regulated posttranscriptionally by the synergistic action of auxin and cytokinin in association with progression of the TE differentiation program.

Localization of the *ZeXYP1* transcripts and xylogen were investigated by *in situ* hybridization (Fig. 3e–h) and immunohistochemistry (Fig. 3i–m), respectively. The *ZeXYP1* transcripts and xylogen were abundant in procambium and immature xylem cells of the *Zinnia* stems but were hardly detected in interfascicular fibres and phloem cells (Fig. 3e–l). Xylogen started to accumulate in the shoot apical meristem (Fig. 3m). Details of xylogen localization were further analysed by indirect fluorescent antibody technique with longitudinal sections. In the immature xylem, xylogen had a polar localization on the apical side of the cell walls of differentiating TEs (Fig. 3n, o), implying that premature TEs secrete xylogen in a polar manner to act on neighbouring cells directionally. The polar localization of xylogen may involve the function of the GPI anchor, because xylogen proteins have a putative GPI-anchor attachment site and GPI anchors direct an uneven distribution of protein in various GPI-anchored proteins[16,17].

Transfer-DNA (T-DNA) insertion mutants of *AtXYP1* or *AtXYP2* were analysed to define the function of xylogen during xylem development *in planta* (Fig. 4). We identified three lines in the SIGnAL database[18] with T-DNA insertions into *AtXYP1* (salk_073673, salk_103127 and salk_147826) and two lines with insertions into *AtXYP2* (salk_055597 and salk_122768). In addition, *xyp2-3* was identified from the Tag-line pool of the Kazusa DNA Research Institute. Although the locations of the T-DNA inserts were confirmed by polymerase chain reaction (PCR) and sequencing, none of the insertion mutants showed obvious defects in morphology. To determine whether *AtXYP1* and *AtXYP2* function redundantly, we analysed the double knockout mutants *xyp1-1 xyp2-2* and *xyp1-2 xyp2-1*. These mutants showed no detectable accumulation of *AtXYP1* and *AtXYP2* transcripts (Fig. 4b), indicating that the insertions created null mutations. More notably, the double knockouts had obvious morphological defects in vascular development as compared with the wild type (Fig. 4c–n).

The digenic knockouts induced discontinuous and thicker veins (Fig. 4d–f) and the improper interconnection of TEs (Fig. 4h). Some TEs differentiated separately from the xylem vessel networks (Fig. 4h). In addition, there was a reduction in the vein loop architecture in the double mutants. In rosette leaves, the number of tertiary veins was markedly reduced and loop formation was severely impaired, resulting in a simpler venation pattern similar to the open venation of ferns and gymnosperms (Fig. 4i–l). In some seedlings of the double knockouts, disconnection of vessels was found in roots as well as in cotyledons and leaves (Fig. 4m, n).

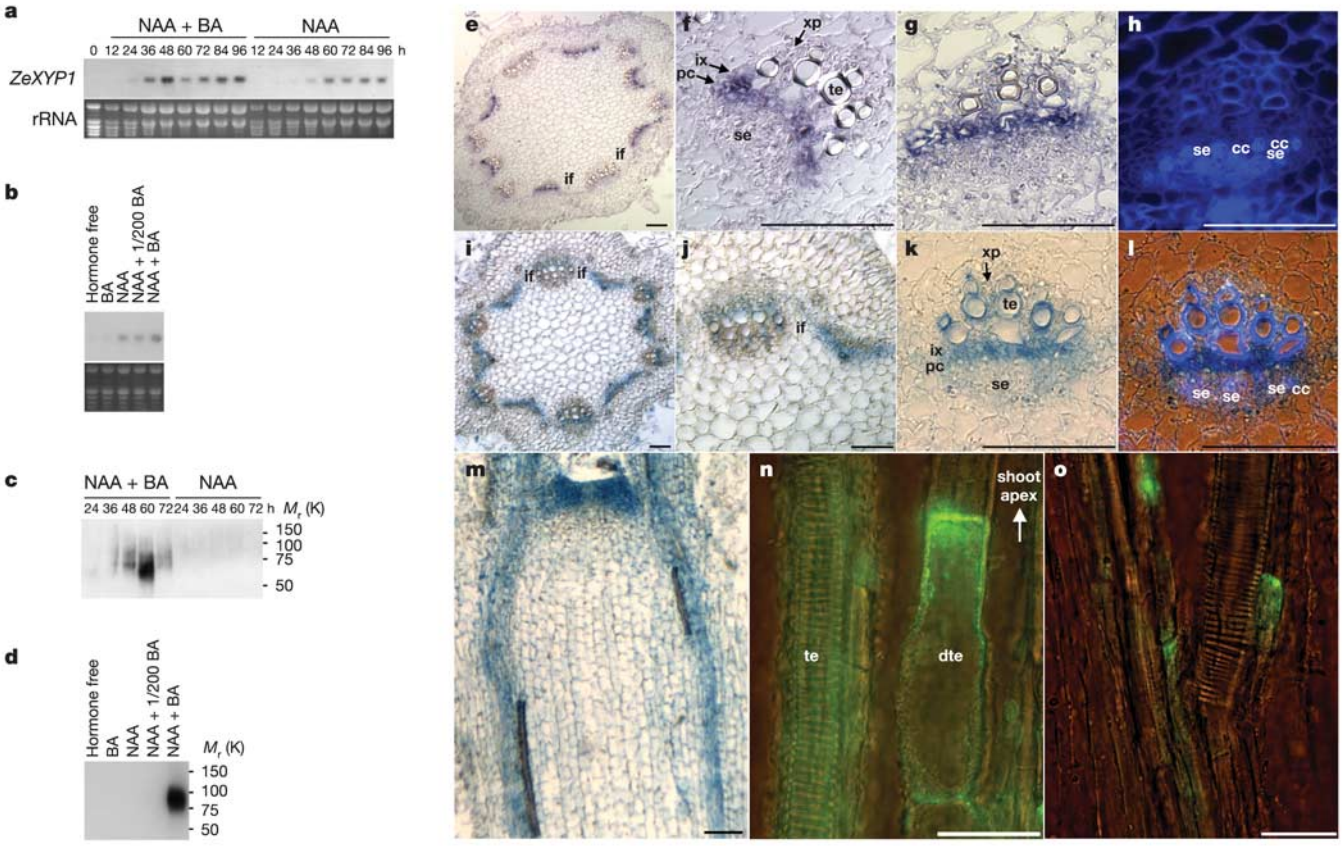

Figure 3 Temporal and spatial profiles of xylogen expression. **a**–**d**, RNA gel blot analyses of *ZeXYP1* (**a**, **b**) and protein gel blot analyses of xylogen (**c**, **d**) in xylogenic (NAA plus BA) and non-xylogenic (hormone free, BA, NAA, NAA plus 1/200 BA) culture. NAA, 0.1 μg ml^{-1} 1-naphthaleneacetic acid; BA, 0.2 μg ml^{-1} 6-benzyladenine; 1/200 BA, 0.001 μg ml^{-1} 6-benzyladenine. **e**–**h**, *ZeXYP1* transcripts accumulate in procambium and immature xylem cells, as visualized by *in situ* hybridization on a cross-section of a 14-day-old *Zinnia* seedling. **f**, **g**, Higher magnification images of **e**. **h**, Ultraviolet image of **g**. **i**–**m**, Immunohistochemical localization of xylogen in procambium and immature xylem cells of 14-day-old *Zinnia* seedling. **j**, **k**, Higher magnification images of **i**. **l**, Ultraviolet image of **k**. **m**, A longitudinal section. **n**, **o**, Localization of xylogen by an indirect fluorescent antibody technique. Scale bars, 100 μm (**e**–**l**), 50 μm (**m**) and 20 μm (**n**, **o**). cc, companion cell; dte, differentiating TE; if, interfascicular fibre; ix, immature xylem cells; pc, procambium; se, sieve element; te, TE; xp, xylem parenchyma cell.

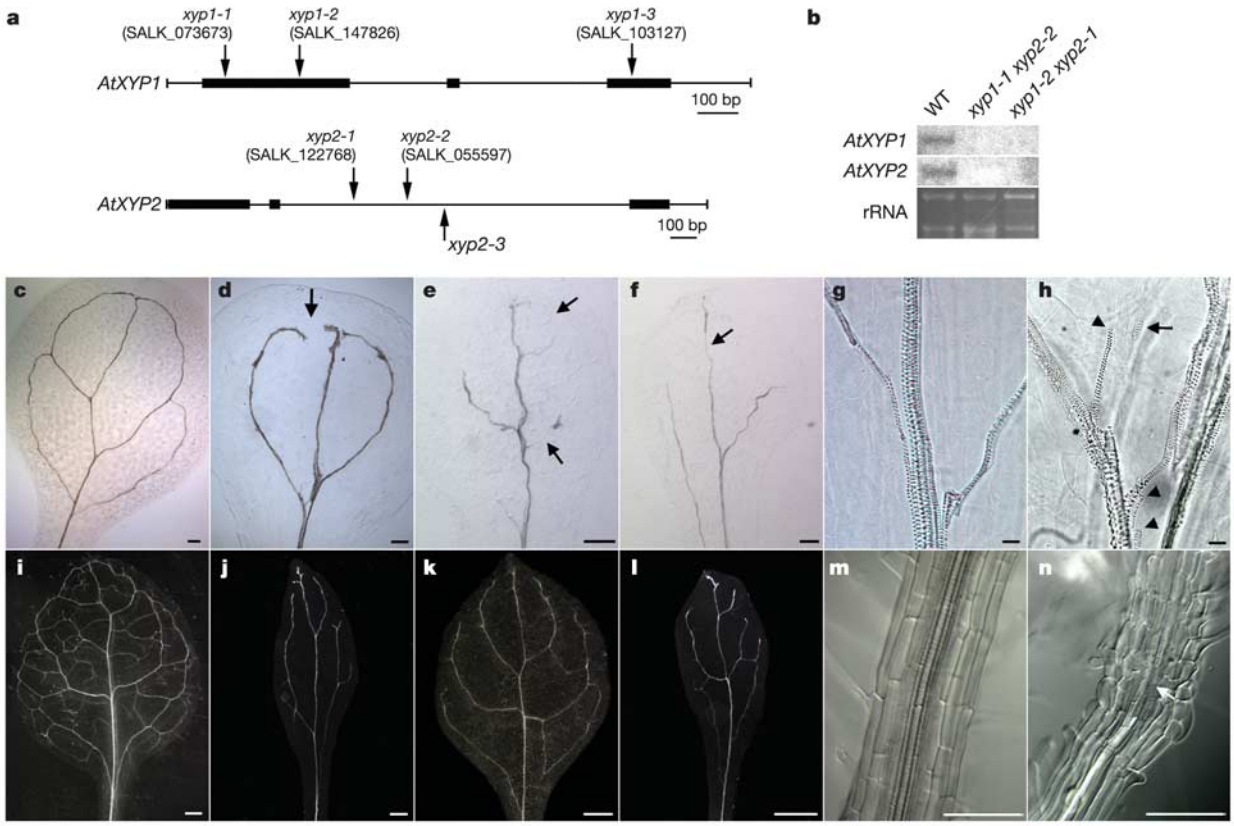

Figure 4 Phenotypic analysis of *Arabidopsis* xylogen knockouts. **a**, Exon–intron structures of *AtXYP1* and *AtXYP2* showing positions of T-DNA in insertion mutants. **b**, The double knockouts (*xyp1-1 xyp2-2* and *xyp1-2 xyp2-1*) completely abolished expression of both *AtXYP1* and *AtXYP2*. WT, Wild type. **c**–**h**, Vascular patterns of a cotyledon of wild type (**c**, **g**), *xyp1-1 xyp2-2* (**d**, **h**), *xyp1-2 xyp2-1* (**e**) and *xyp1-1 xyp2-3* (**f**) grown for 8 d. **g**, **h**, Higher magnification images of **c**, **d**, respectively. Shown are discontinuous veins (**d**–**f**, arrows), separated TE (**h**, arrow) and wrongly interconnected vessels (**h**, arrowheads). **i**–**l**, Vascular patterns of a rosette leaf of wild type (**i**), *xyp1-1 xyp2-2* (**j**), *xyp1-2 xyp2-1* (**k**) and *xyp1-1 xyp2-3* (**l**) grown for 22 d. **m**, **n**, Vascular patterns of a root of wild type (**m**) and *xyp1-1 xyp2-2* (**n**) grown for 8 d. Discontinuous vessel (**n**, arrow). Bars, 200 μm (**c**–**f**), 20 μm (**g**, **h**), 500 μm (**i**–**l**) and 100 μm (**m**, **n**).

Similar phenotypic characters were also observed in *xyp1-1 xyp2-3* (Fig. 4f, l). These results, together with the data obtained with the *in vitro* system, indicate that xylogen may function as a mediator of inductive cell–cell interaction in vascular development.

It should be noted, however, that xylogen seems not to be an essential component of the basic machinery responsible for vascular tissue differentiation, because a deficiency of xylogen did not cause a total loss of vascular tissues but had an influence on limited aspects of vascular development, and in some organs its effect was insignificant. For example, no apparent changes in the vascular structure were detected in hypocotyls of seedlings of the xylogen double knockouts and, in the inflorescence stems of mature plants of the double knockouts, the xylem area was only slightly diminished (data not shown). Thus, we consider that xylogen has the role of a coordinator, rather than a determinant, during vascular development to generate minor veins and to guarantee the integrity of vascular networks.

In summary, our findings on xylogen suggest a scheme in which xylogen is secreted directionally from differentiating vascular cells, moves in the apoplast to the adjacent undifferentiated cells and draws them into the pathway of vascular differentiation to support the formation of continuous networks of vasculature. In addition, the simplified venation in the xylogen double knockouts and the accumulation of xylogen in the meristem suggest that xylogen is involved in the pattern formation of procambial tissues. The phenotype of the xylogen double knockouts reminds us of several *Arabidopsis* mutants that show discontinuous veins[19,20]. Among these mutants with discontinuous vasculature, *cotyledon vascular pattern1* (*cvp1*) is notable in consideration of the function of xylogen[21]. Because *CVP1* encodes sterol methyltransferase 2, an enzyme involved in the biosynthesis pathway of sitosterol and stigmasterol, sterols or sterol-derived molecules are implicated in vascular development as patterning signals[21]. The sterol-binding ability of xylogen, together with the findings on *CVP1*, raises the possibility that xylogen functions as a complex with a type of sterol or sterol-derived molecule. □

Methods

Cell culture

Asparagus mesophyll cells were isolated and cultured as described[22]. We counted TEs under a light microscope at the tenth day of culture. The frequency of TE differentiation was calculated as the proportion of TEs to the number of living cells. Microbead cultures and suspension cultures of *Zinnia* mesophyll cells were done as described[3]. The xylogenic culture medium for the induction of TE differentiation contained auxin (0.1 μg ml^{-1} 1-naphthaleneacetic acid; NAA) and cytokinin (0.2 μg ml^{-1} 6-benzyladenine; BA). The non-xylogenic media contained four different combinations of auxin and cytokinin: no hormones; 0.2 μg ml^{-1} BA; 0.1 μg ml^{-1} NAA; or 0.1 μg ml^{-1} NAA and 0.001 μg ml^{-1} BA.

We monitored the activity of xylogen with microbead cultures[3], in which *Zinnia* mesophyll cells were embedded in bead-shaped agarose gels at a cell density of 2.5×10^4 cells per ml (low density) or 8.0×10^5 cells per ml (high density). Low-density and high-density microbeads were cultured together to give a total cell density of 2.2×10^4 cells per ml in the liquid xylogenic medium containing various concentrations of xylogen and deglycosylated xylogen. In the suspension cultures, *Zinnia* mesophyll cells were cultured at a cell density of 8.0×10^4 cells per ml in the liquid media. We counted TEs under a light microscope at 96 h of culture. The frequency of TE differentiation was calculated as the proportion of TEs to the number of living cells. Values and error bars are the means and standard deviations, respectively, of triplicate measurements.

To overexpress xylogen proteins, chimaeric genes composed of the cauliflower mosaic virus 35S promoter and the ORF of ZeXYP1, AtXYP1 or AtXYP2 were introduced into tobacco BY-2 cells by *Agrobacterium*-mediated transformation[23]. BY-2 cells transformed

with empty vector were used as controls. We isolated AGP fractions from the culture medium of transgenic BY-2 cells by using the specific interaction of AGPs with βGlcY[3] and added them into *Zinnia* microbead cultures to monitor the activity of xylogen.

Analysis of xylogen

Xylogen was purified from the AGP fraction, which was obtained from the conditioned medium of the *Zinnia* xylogenic culture by using the specific interaction of AGPs with βGlcY[3]. The AGP fraction was boiled for 10 min and centrifuged at 10,000 *g* for 20 min. The supernatant was applied onto concanavalin-A–sepharose column (Amersham Pharmacia Biotech) equilibrated with 10 mM KH_2PO_4-KOH (pH 7.2) containing 150 mM NaCl. The column was washed with the same buffer, and xylogen was eluted with the same buffer containing 0.2 M methyl-α-D-glucoside. Purified xylogen was deglycosylated by trifluoromethanesulphonic acid[24]. The resulting 16K polypeptide was sequenced by a G1005A Protein Sequencing System (Hewlett Packard) according to the manufacturer's protocol.

For 3′-RACE, the first strand cDNA was reverse-transcribed from poly(A)$^+$ RNA prepared from cultured *Zinnia* cells with dT17-LL-BamA primer (GATTAGGATCCAC $TAATATCT_{17}$). A degenerate primer F1 (GCNCAYCARACIGGIGCICCIGCICCI) was designed for the N-terminal amino acid sequence of the 16K protein backbone of xylogen. A cDNA fragment was amplified from the first strand cDNA by PCR with the primer set F1 and LL-BamA (GATTAGGATCCACTAATATC). DNA of 0.5 kilobase pairs (kbp) was cloned and sequenced. On the basis of the nucleotide sequences of cDNA fragments obtained through 3′-RACE, a backward primer R2 (CCACAATTAGTAGCCAGAAGG AGC) was designed for 5′-RACE. First strand cDNA was synthesized from poly(A)$^+$ RNA with the R2 primer, and subjected to dC-tailing reaction. PCR amplification from dC-tailed cDNA was done with a primer set, R2 and poly(G)-AP (GGCCACGCGTCGACT AGTACGGGIIGGGIIGGGIIG) to yield DNA of 0.4 kbp, which was cloned and sequenced.

We carried out the protein–lipid overlay assay as described[15]. Nitrocellulose membranes with spots of lipids and sterols were incubated with 0.5 μg ml^{-1} xylogen or deglycosylated xylogen. The membranes were incubated first with antibody against ZeXYP1 and then with a peroxide-conjugated secondary antibody.

Expression and localization analysis

RNA gel blot analysis, immunoblotting, *in situ* hybridization and immunohistochemistry were done as described[25]. A rabbit antibody against ZeXYP1 was generated against a synthetic peptide of ZeXYP1 (CLSYVTAGSTVKKPEGT) and purified with affinity chromatography. Monoclonal antibody JIM13 was a gift from K. Roberts (John Innes Centre). We purchased polyclonal antibodies against plasma membrane intrinsic protein 2a (PIP2a) and KNOLLE from Rose Biotechnology. Alkaline phosphatase (AP)-labelled dextran polymer conjugated with anti-rabbit Ig (EnVision/AP, DakoCytomation) and fluorescein isothiocyanate (FITC)-conjugated anti-rabbit Ig (Sigma-Aldrich) were used as the secondary antibodies. The antigen–EnVision/AP complex was detected by an AP Substrate kit (Vector Laboratories).

T-DNA insertion mutants

xyp1-1 (salk_073673), *xyp1-2* (salk_147826), *xyp1-3* (salk_103127), *xyp2-1* (salk_122768) and *xyp2-2* (salk_055597) were provided from SIGnAL. Information about these mutants was obtained from the SIGnAL website (http://signal.salk.edu). *xyp2-3* (the Landbeg *erecta* ecotype), identified from the Tag-line pool of the Kazusa DNA Research Institute, was a gift from A. Nagatani (Kyoto University). We analysed the vascular patterns of wild type and T-DNA mutants as described[20].

Received 19 January; accepted 4 May 2004; doi:10.1038/nature02613.

1. Van Den Berg, C., Willemsen, V., Hage, W., Weisbeek, P. & Scheres, B. Cell fate in the *Arabidopsis* root meristem determined by directional signalling. *Nature* **378,** 62–65 (1995).
2. Motose, H., Fukuda, H. & Sugiyama, M. Involvement of local intercellular communication in the differentiation of zinnia mesophyll cells into tracheary elements. *Planta* **213,** 121–131 (2001).
3. Motose, H., Sugiyama, M. & Fukuda, H. An arabinogalactan protein(s) is a key component of a fraction that mediates local intercellular communication involved in tracheary element differentiation of zinnia mesophyll cells. *Plant Cell Physiol.* **42,** 129–137 (2001).
4. Fukuda, H. & Komamine, A. Establishment of an experimental system for the study of tracheary element differentiation from a single cell isolated from the mesophyll of *Zinnia elegans*. *Plant Physiol.* **65,** 57–60 (1980).
5. Fukuda, H. Tracheary element differentiation. *Plant Cell* **9,** 1147–1156 (1997).
6. Yates, E. A. *et al.* Characterization of carbohydrate structural features recognized by anti-arabinogalactan-protein monoclonal antibodies. *Glycobiology* **6,** 131–139 (1996).
7. Anderson, R. L., Clarke, A. E., Jermyn, M. A., Knox, R. B. & Stone, B. A. A carbohydrate-binding arabinogalactan protein from liquid suspension cultures of endosperm from *Lolium multiflorum*. *Aust. J. Plant Physiol.* **4,** 143–158 (1977).
8. Komalavilas, P., Zhu, J.-K. & Nothnagel, E. A. Arabinogalactan-proteins from the suspension culture medium and plasma membrane of rose cells. *J. Biol. Chem.* **266,** 15956–15965 (1991).
9. Yamada, M. Lipid transfer proteins in plants and microorganisms. *Plant Cell Physiol.* **33,** 1–6 (1992).
10. Kader, J. C. Lipid-transfer proteins in plants. *Annu. Rev. Plant Physiol. Plant Mol. Biol.* **47,** 627–654 (1996).
11. Youl, J. J., Bacic, A. & Oxley, D. Arabinogalactan-proteins from *Nicotiana alata* and *Pyrus communis* contain glycosylphosphatidylinositol membrane anchors. *Proc. Natl Acad. Sci. USA* **95,** 7921–7926 (1998).
12. Oxley, D. & Bacic, A. Structure of the glycosylphosphatidylinositol anchor of an arabinogalactan protein from *Pyrus communis* suspension-cultured cells. *Proc. Natl Acad. Sci. USA* **96,** 14246–14251 (1999).
13. Svetek, J., Yadav, M. P. & Nothnagel, E. A. Presence of a glycosylphosphatidylinositol lipid anchor on rose arabinogalactan proteins. *J. Biol. Chem.* **274,** 14724–14733 (1999).
14. Nothnagel, E. A. Proteoglycans and related components in plant cells. *Int. Rev. Cytol.* **174,** 195–291 (1997).
15. Stevenson, J. M., Perera, I. Y. & Boss, W. F. A phosphatidylinositol 4-kinase pleckstrin homology domain that binds phosphatidylinositol 4-monophosphate. *J. Biol. Chem.* **273,** 22761–22767 (1998).
16. Rodriguez-Boulan, E. & Powell, S. K. Polarity of epithelial and neuronal cells. *Annu. Rev. Cell Biol.* **8,** 395–427 (1992).
17. Schindelman, G. *et al.* COBRA encodes a putative GPI-anchored protein, which is polarly localized and necessary for oriented cell expansion in *Arabidopsis*. *Genes Dev.* **15,** 1115–1127 (2001).
18. Alonso, J. M. *et al.* Genome-wide insertional mutagenesis of *Arabidopsis thaliana*. *Science* **301,** 653–657 (2003).
19. Berleth, T. & Mattsson, J. Vascular development: tracing signals along veins. *Curr. Opin. Plant Biol.* **3,** 406–411 (2000).
20. Koizumi, K., Sugiyama, M. & Fukuda, H. A series of novel mutants of *Arabidopsis thaliana* that are defective in the formation of continuous vascular network: calling the auxin signal flow canalization hypothesis into question. *Development* **127,** 3197–3204 (2000).
21. Carland, F. M., Fujioka, S., Takatsuto, S., Yoshida, S. & Nelson, T. The identification of *CVP1* reveals a role for sterols in vascular patterning. *Plant Cell* **14,** 2045–2058 (2002).
22. Matsubayashi, Y. & Sakagami, Y. Phytosulfokine, sulfated peptides that induce the proliferation of single mesophyll cells of *Asparagus officinalis* L. *Proc. Natl Acad. Sci. USA* **93,** 7623–7627 (1996).
23. Ito, M. *et al.* A novel *cis*-acting element in promoters of plant B-type cyclin genes activates M phase-specific transcription. *Plant Cell* **10,** 331–341 (1998).
24. Sojar, H. T. & Bahl, O. P. Chemical deglycosylation of glycoproteins. *Methods Enzymol.* **138,** 341–359 (1987).
25. Nishitani, C., Demura, T. & Fukuda, H. Primary phloem-specific expression of a *Zinnia elegans* Homeobox gene. *Plant Cell Physiol.* **42,** 1210–1218 (2001).

Acknowledgements We thank J. J. Harada for critically reading the manuscript; K. Roberts for JIM13; S. Hasezawa and T. Nagata for tobacco BY-2 cells; S. Sawa for advice on the protein–lipid overlay assay; N. Sassa, K. Iwamoto and C. Nishitani for advice on *in situ* hybridization; M. Fujita and N. Shinohara for advice on immunohistochemistry; the Salk Institute Genomic Analysis Laboratory for the sequence-indexed *Arabidopsis* T-DNA insertion mutants; the Kazusa DNA Research Institute for the Tag-line pool; A. Nagatani for *xyp2-3* seeds; K. Ohashi-Ito and S. Sakamoto for the screening and isolation of *xyp2-3*. H.M. was supported in part by the Yamada Science Foundation. Funding for the SIGnAL indexed insertion mutant collection was provided by the National Science Foundation of USA. This work was supported in part by Grants-in-Aid from the Ministry of Education, Science, Sports and Culture of Japan, from the Japan Society for the Promotion of Science, and from the Mitsubishi Foundation.

Competing interests statement The authors declare that they have no competing financial interests.

Correspondence and requests for materials should be addressed to H.M. (hmotose@ucdavis.edu).
The sequence for ZeXYP1 is deposited in GenBank under accession number AB159560.

Rapid BDNF-induced retrograde synaptic modification in a developing retinotectal system

Jiu-lin Du & Mu-ming Poo

Division of Neurobiology, Department of Molecular and Cell Biology, Helen Wills Neuroscience Institute, University of California, Berkeley, California 94720, USA

In cultures of hippocampal neurons, induction of long-term synaptic potentiation or depression by repetitive synaptic activity is accompanied by a retrograde spread of potentiation or depression, respectively, from the site of induction at the axonal outputs to the input synapses on the dendrites of the presynaptic neuron[1,2]. We report here that rapid retrograde synaptic modification also exists in an intact developing retinotectal system. Local application of brain-derived neurotrophic factor (BDNF) to the *Xenopus laevis* optic tectum, which induced persistent potentiation of retinotectal synapses, led to a rapid modification of synaptic inputs at the dendrites of retinal ganglion cells (RGCs), as shown by a persistent enhancement of light-evoked excitatory synaptic currents and spiking activity of RGCs. This retrograde effect required TrkB receptor activation, phospholipase Cγ activity and Ca^{2+} elevation in RGCs, and was accounted for by a selective increase in the number of postsynaptic AMPA-subtype glutamate receptors at RGC